CFD ANALYSES OF THE INTERNAL BLOCKAGE IN THE NACIE-UP FUEL PIN BUNDLE SIMULATOR

I. Di Piazza
ENEA FSN-ING
Brasimone R.C., Camugnano (Bo), 40033, Italy
ivan.dipiazza@enea.it

R. Marinari , N. Forgione
DICI
University of Pisa
Largo Lucio Lazzarino 2, 56122 Pisa (Italy)
ranieri.marinari@ing.unipi.it , nicola.forgione@ing.unipi.it

F. Magugliani
Department of Engineering Physics
University of Wisconsin-Madison
1500 Engineering Drive, Madison, WI 53706, USA
fabriziomagugliani@yahoo.com

W. Borreani
DIME-Thermal Division
University of Genoa
Via all'Opera Pia 15, 16145 Genova, Italy
walter.borreani@unige.it

H. Doolaard, F. Roelofs
NRG
Westerduinweg 3, 1755 LE, Petten, Netherlands
doolaard@nrg.eu , roelofs@nrg.eu

F. Piscaglia, A. Montorfano
Dipartimento di Energia
Politecnico di Milano
via Lambruschini 4, 20156 Milano, Italy
federico.piscaglia@polimi.it , andrea.montorfano@polimi.it

V. Moreau
CRS4
Science and Technology Park Polaris – Piscina Manna, 09010 Pula, Italy
moreau@crs4.it

ABSTRACT

In the context of GEN-IV heavy liquid metal-cooled reactors safety studies, the flow blockage in a fuel sub-assembly is considered one of the main issues to be addressed and one of the most important accidents for Lead Fast Reactors (LFR). In order to model the temperature and velocity field inside a wrapped fuel assembly under unblocked and blocked conditions, a detailed experimental campaign as well as 3D thermal hydraulic analyses of the fuel assembly are required.

The present paper is focused on the CFD modelling and preliminary computational analysis of the new experimental facility 'Blocked' Fuel Pin bundle Simulator (BFPS) that will be inserted in the heavy liquid metal NACIE-UP (NAtural CIrculation Experiment-UPgrade) facility located at the ENEA Brasimone Research Center (Italy). The BFPS test section aims to carry out suitable experiments to fully investigate different flow blockage regimes in a 19-pin fuel bundle providing experimental data in support of the development of the ALFRED (Advanced Lead-cooled Fast Reactor European Demonstrator) LFR DEMO. The BFPS test section, cooled by lead bismuth eutectic, was conceived with a thermal power of about 250 kW and a wall heat flux up to 0.7 MW/m^2, which are relevant values for a LFR. It consists of 19 grid-spaced electrical pins placed on a hexagonal lattice with a pitch to diameter ratio of 1.4 and a diameter of 10 mm.

The geometrical domain of the fuel pin bundle simulator was designed to reproduce the geometrical features of ALFRED, e.g. the external wrapper in the active region and the spacer grids.

Different modelling approaches (e.g. meshing, turbulence modelling, codes and users) in RANS, URANS and LES will be compared to each other. The pre-test analyses presented here will facilitate the post-test analysis of the experimental data expected in 2017-2018. These calculations were carried out by applying unambiguous boundary conditions. In addition conjugate heat transfer is also considered.

The comparison among different codes and turbulence models allows to make an overall assessment of different approaches to CFD modelling and simulation. ANSYS CFX, ANSYS FLUENT, STAR-CCM+ and OpenFoam simulations are compared to each other.

KEYWORDS

Heavy Liquid Metal, CFD, Flow Blockage

1. INTRODUCTION

The flow blockage accident in a fuel assembly (FA) of a nuclear reactor consists of a partial or total occlusion of the flow passage area. This leads in general to a degradation of the heat transfer. The root causes of the FA blockage are aggregation of solid matter (oxides), dislodged from its intended location or generated in the coolant, transported inside and along with the coolant's flow; this matter could stop inside the FA (mainly because of its narrow spaces) and interfere with the coolant flowing inside the FA. The main consequence of the blockage is a reduction of the coolant flow rate through the FA leading to rising temperatures.

FAs are usually designed with a number of inlets slots to prevent a complete and instantaneous blockage. Blockage can be instantaneous (when a large enough piece of material obstructs a portion of the channels of the FA) or time dependent (when the aggregation of solid matter piles up in the channels of the FA). For grid-spaced FAs, an internal blockage is most probable to be located in the first grid and it has a flat-like shape. Regarding the sodium fast reactors, wire-spaced bundles are generally adopted, and the accumulation of debris from failed fuel pins or broken wires might occur along the wire. Therefore, in this case, the preferential shape of the blockage is elongated and it follows the helicoid wire [1].

Fuel Assembly blockage (total or partial) has been extensively analysed since the early days of fast reactors. While many of these studies refer to Sodium Fast Reactors, the results may be a starting point for LFRs to. The main focus of these analyses is determining the effects of a blockage on the temperature (cladding and coolant) and pressure (coolant) inside the FA as well as at the outlet of the subassembly, and the optimal detection techniques.

Seung-Hwan Seong et al. [2] used the LES turbulence model in the ANSYS CFX code for analyzing the temperature fluctuation in the upper plenum. After analyzing the temperature fluctuations in the upper plenum, a basic design requirement was established for the flow blockage detection system through a FFT analysis and a statistical analysis. They concluded that response time of a measuring device should be less than 13ms and that it should cover a high temperature range of 1000 K. In addition, the resolution of the thermocouple should be less than 2 K and its location should be within 25 cm from the exit of each assembly.

Maity et al. [3] carried out thermal hydraulic studies to understand temperature dilution experienced by a core-temperature monitoring system of a sodium cooled fast reactor. The three-dimensional computational model is validated against experimental results of a water model. The analysis indicates the maximum possible dilution in fuel and blanket subassemblies to be 2.63 K and 46.84 K, respectively. Shifting of thermocouple positions radially outward by 20 mm with respect to subassembly centers leads to an overall improvement in accuracy of thermocouple readings. It is also seen that subassembly blockage that leads to 7% flow reduction in fuel subassembly and 12% flow reduction in blanket subassembly can be detected effectively by the core-temperature monitoring system.

Di Piazza et al. [4] carried out a CFD study on fluid flow and heat transfer in the Lead-cooled Fuel Pin Bundle of the ALFRED LFR DEMO. The authors developed a detailed thermo-fluid dynamic analysis at various levels of geometrical blockage. In particular the closed hexagonal, grid-spaced fuel assembly of the LFR ALFRED was modeled and computed. While the spacer grids were not included in the model, a conservative analysis has been carried out based on the current main geometrical and physical features. Results indicate that critical conditions, with clad temperatures $\approx 900^{\circ}$ C, are reached with geometrical blockage larger than 30% in terms of area fraction. The results show that two main effects can be distinguished: a local effect in the wake/recirculation region downstream the blockage and a global effect due to the lower mass flow rate in the blocked subchannels; the former effect gives rise to a temperature peak behind the blockage and it is dominant for large blockages (>20 %), while the latter effect determines a temperature peak at the end of the active region and it is dominant for small blockages (<10 %).

The present paper is focused on a CFD preliminary computational analysis of the new experimental facility 'Blocked' Fuel Pin bundle Simulator (BFPS) that will be inserted in the heavy liquid metal NACIE-UP (NAtural CIrculation Experiment-UPgrade) facility located at the ENEA Brasimone R.C. (Italy) as fully described in [5]. The BFPS test section will provide experimental data in support of the development of the ALFRED (Advanced Lead-cooled Fast Reactor European Demonstrator) LFR DEMO [6] for internal blockage.

Different modeling approaches (e.g. meshing, turbulence modelling, codes and users) in RANS, URANS and LES will be compared to each other. The pre-test analyses presented here will facilitate the post-test analysis of the experimental data expected in 2017-2018.

The comparison among different codes (ANSYS CFX -Unipi/ENEA-, STAR-CCM+ -NRG&CRS4, UniGe-, OpenFoam -PoliMi-) and turbulence models allows to make an overall assessment of different approaches to CFD modeling.

2. THE BFPS TEST SECTION

The Blockage Fuel Pin Simulator (BFPS) test section was designed in order to study the local and bulk effects of an internal blockage in a 19-pin LFR ALFRED DEMO-like FPS.

The heat source will consist of 19 electrical pins with an active length L_{active} = 600 mm (L_{total} = 2000 mm, including the *non-active* length) and a diameter D= 10 mm. The pitch to diameter ratio is P/D=1.4. The maximum external wall pin heat flux will be ≈0.7 MW/m^2. The pins will be placed on a hexagonal layout by a suitable wrapper, while two grids will maintain the pin bundle in the correct position, the total power of the pin fuel bundle is ≈ 250 kW.
This fuel pin bundle configuration is relevant for the ALFRED's core thermal-hydraulic design. ALFRED is a flexible fast spectrum research reactor (300 MW_{th}). The main parameters of BFPS test section and ALFRED core are reported in Table 1 for comparison.

Parameter	BFPS	ALFRED FA	Definition
d_{pin}[mm]	10	10.5	Pin outer diameter
p/d_{pin}	1.4	1.32	Pitch to diameter ratio
Q [kW]	250	-	Total power
Q_{pin} [kW]	13	-	Pin power
q'' [MW/m^2]	0.7	0.7-1	Heat flux
v [m/s]	0.8	1.1	Subchannel velocity
N_{pins}	19	127	Number of pins per FA
L_{active} [mm]	600	600	Active length
L_{plenum} [mm]	500	500	FA mixing region

Table 1 Comparison of the main parameter between the BFPS test section and ALFRED core

The goals of the experimental campaigns planned on the NACIE-UP loop facility with the BFPS bundle are:

- measurement of the pin wall temperature both with and without blockage by embedded thermocouples;
- measurement of the subchannel temperature;
- Heat Transfer Coefficient (HTC) evaluation;
- axial temperature profiles in the wrapper and in the subchannels;
- check the presence of hot spots and localized peak of temperature;
- evaluation of the thermal mixing above the pin bundle (BFPS);

A drawing of the BFPS test section is shown in Figure 1. A spacer grid is located at the beginning of the active region where the coupling flange is present. Without blockage, the test section allows to characterize the flow and the heat transfer in the FA.
Proper experiments were designed in order to describe the thermal-hydraulic behavior of a simplified version of FA during internal flow blockage accident, simulated by blocking some holes of the first spacer grid (at the beginning of the heated length) with appropriate caps.
The central spacer grid will be the key component of the flow blockage experimental campaign and it is specifically described in the following.
The central grid in its different configurations is shown (viewed from the top) in Figure 2. For the flow blockage configurations, several caps will be displaced on the different holes of the central grid, those

caps will be small thin plates of appropriate shape positioned by moving rods from the bottom to fix a configuration. The test section will be instrumented with more than 100 thermocouples located both in the heated region and in the mixing one.

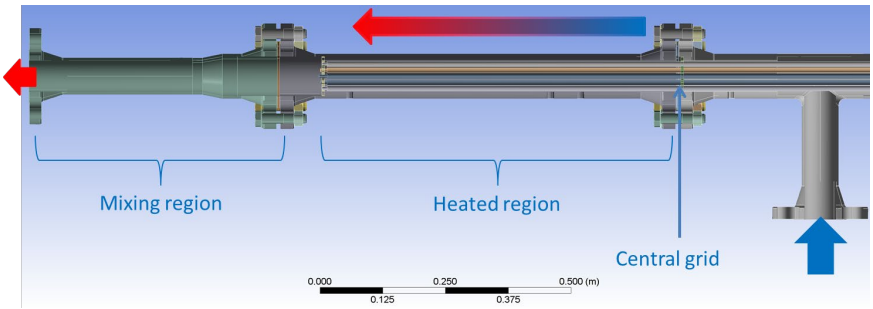

Figure 1 Sketch of the BFPS test section.

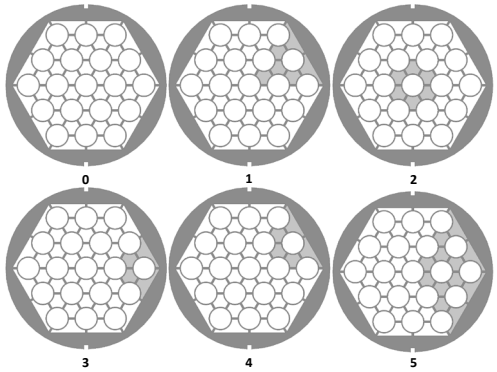

Figure 2 Sketch of the central grid: unblocked (0) and at different degree of blockage (viewed from the top)

The thermocouples locations are shown in Figure 3, with the instrumented pins colored in red. Pins 1, 2, 5, 15 will be equipped with wall embedded thermocouples on a generatrix parallel to the pin axis, and sub-channel B2 will be instrumented with 0.5 mm bulk thermocouple. The diameter of the wall embedded thermocouples is 0.35 mm.

Sixteen different levels will be considered for the four generatrices and the sub-channel: z= 10, 20, 30, 40, 50, 60, 70, 80, 90, 100, 150, 200, 300, 400, 500, 600 mm starting from the beginning of the active region of the pins. Plane at z= 550 mm will be instrumented as in the following to characterize the heat transfer in the unblocked case:

- pins 1, 2, 4, 5, 7, 9, 14, 15 will be instrumented with wall embedded thermocouples;
- sub-channels B1, B2, B5, E1, E5 and the corner sub-channels across B5/C4 and E5/F4 will be instrumented with bulk thermocouples 0.5 mm thickness placed at the center of the subchannel;
- An additional bulk thermocouple of 0.35 mm thickness is placed in subchannel B1 at a distance of 1 mm from the wall.

This instrumentation will allow to collect data on temperature distribution in the case of blockage and to characterize the heat transfer in the unblocked condition by measuring cold spots in the side subchannels and the heat transfer coefficients.

Additional instrumentation (24 TCs) will be placed in the 500 mm mixing region of the test section to collect data for CFD code validation and LBE thermal mixing. TCs will be placed downstream the FPS at different axial, radial and azimuthal positions.

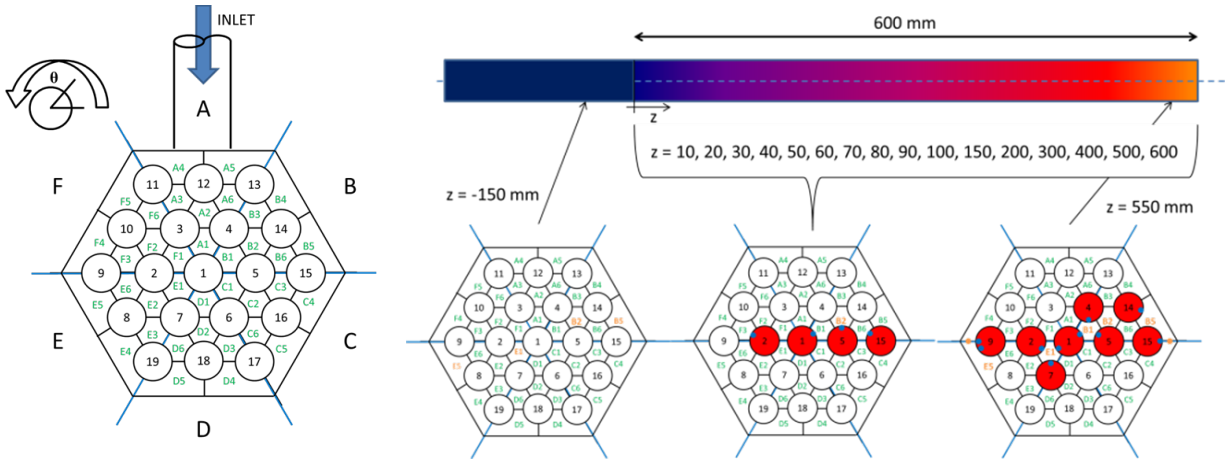

Figure 3 Pin and subchannels nomenclature (left); Overall pin bundle TCs instrumentation (right)

3. MODELS AND METHODS

3.1 Geometry and boundary conditions

The computational domain is fixed for all the partners and shown in Figure 4-left-. It includes (from bottom to top) the bend region, the heated region, and the mixing region downstream of the BFPS. The origin of the global reference system is placed on the center of the upper surface of the central grid (z axis pointing to the mixing region).

The conjugate heat transfer in the 19 pins, the hexagonal wrapper, the upper tube and the coupling flanges was also considered. The importance of the conjugate heat transfer in this kind of test sections was already assessed in previous works, see [7] and [8]. Constant mass flow rate, temperature at inlet and pressure at outlet were applied for the simulations. The external surfaces of pipes and flanges are considered adiabatic, being insulated with 100 mm of thermal insulator.

A summary of the boundary conditions is reported in Figure 4-right-. The present paper is focused on blockage type 4 (edge blockage) performed on sector B (see Figure 2).

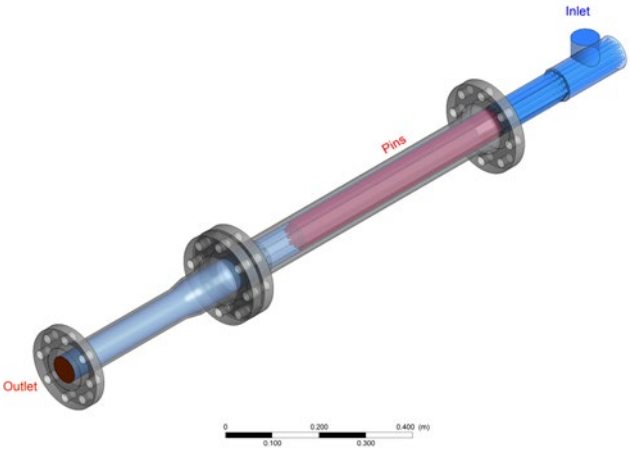

Boundary	Boundary condition	Value
Inlet	Mass flow Temperature	8 kg/s 200 °C
Inner diameter pin clad	Heat flux	156716 W/m^2
Walls (fluid-solid)	Velocity	No-slip
Outlet	Relative pressure	0 bar

Figure 4 Sketch of the computational domain (left) and main boundary conditions adopted (right)

Constant properties of the LBE are assumed, computed at 220°C (average bulk temperature increase into the fluid), based on OECD/NEA handbook [9]. The steel is also assumed to have constant properties, those of steel AISI 304.
The turbulent Prandtl number was set to 2.0, according to literature suggestion [10]. Buoyancy forces were neglected (conservative approach).

3.2Numerical methods

The participants performed Reynolds Averaged Navier-Stokes (RANS) or Unsteady Reynolds Averaged Navier-Stokes (URANS) simulations. A LES simulation was developed by UniGe/CRS4.
The partners developed their mesh following these general constrains:

- The mesh shall have a maximum of 30 million nodes;
- The mesh shall have a wall resolution (y^+) equal or smaller to one (1) on every fluid-solid interface.

Polimi adopted the open-source CFD code OpenFOAM. The total cell count is about 19.8 million cells for the fluid region and 2.5million cells for the solid one. The mesh (Figure 5 (a)) has been generated using snappyHexMesh, the built-in mesh generator of OpenFOAM. Grid structure is based on iterative octree refinement of a fully-hexahedral background mesh. Boundary points of the refined mesh are projected onto the user-supplied surface to obtain a geometry-fitted grid. As a last step, boundary faces are extruded towards the interior of the mesh to have near-wall prismatic layers for the solution of turbulent flows. The resulting mesh has a hex-dominant, hybrid structure. On wall boundaries an average of 5 layers have been extruded with a minimum thickness of 0.1 mm. Turbulence has been simulated using the standard k-ε RANS model.

ENEA/Unipi used the commercial code ANSYS CFX 15.0. The mesh (Figure 5 (b)) is fully unstructured in the heated region and fully structured in all other regions (fluid and solid ones). The mesh contains about 27 million cells in the fluid region and 2.8 million cells in the solid one. The turbulence model adopted is a standard k-ε model.

NRG performed a URANS simulation adopting the commercial finite-volume code Star-CCM+ 11.06. The mesh (Figure 5 (c)) contains 22.4 million cells: 20 million in the fluid and 2.4 million in the solid parts. The main part of the mesh consists of a polyhedral mesh with prism layers. The thin mesher tool available in the code is applied to create the mesh in the solids. A directed mesh is applied in the bottom part below the inlet bend, in the BFPS downstream the recirculation and in the mixing region. The turbulence model adopted is a standard k-ε low Reynolds model. An implicit scheme was adopted for time discretization. The adopted time-step is 14 ms and the total time is 14 s, starting from an initial field obtained with RANS. The results are averaged over the last 5 s.

UniGe/CRS4 performed an URANS calculation with 14 million nodes. The adopted time-step is 0.3 ms and the total time is 20 s, starting from an initial field obtained with RANS. The results are averaged over the last 10 s. The meshing strategy carried out in STARCCM+ V11.04 includes both Automated mesh Method and Direct Mesh Method, in order to develop an unstructured polyhedral mesh in the bend zone and in the structural grid zone. The turbulence model adopted is the standard k-epsilon one.
Adopting the same mesh developed for URANS simulation (Figure 5 (d)), UniGe/CRS4 performed a preliminary LES calculation. The value of the integral length-scales ℓ_0 has been estimated by the following equation

$$\ell_0 \sim \frac{k^{3/2}}{\varepsilon} \tag{1}$$

and the values of k and ε have been calculated by the URANS simulations performed, averaging their value in time for each fluid volume, as reported in Table 2.

Fuid volume	Volume Average of Turbulent Dissipation Rate ε [m²/s³]	Volume Average of Turbulent Kinetic Energy k [m²/s²]	Integral Lenghtscale $\ell_0 \sim k^{3/2}/\varepsilon$ [m]	Re_L $k^{1/2}\,\ell_0/\nu$ [-]	L_{EI} $\ell_0/6$ [m]
bottom_vol	3.E-04	7.E-05	2.E-03	7.E+01	3.E-04
Esa+cyl_layer	1.E-01	3.E-03	1.E-03	3.E+02	2.E-04
Esa_channel	1.E-01	1.E-03	6.E-04	1.E+02	1.E-04
Fluid slice 2 middle low	1.E-01	3.E-03	9.E-04	2.E+02	1.E-04
Fluid slice 3 middle central	6.E-02	1.E-03	6.E-04	8.E+01	9.E-05
Fluid slice 4 middle up	6.E-02	1.E-03	5.E-04	7.E+01	8.E-05
fluid_slice_1_new	8.E-02	1.E-03	4.E-04	6.E+01	7.E-05
Intersect spacer lower	4.E-01	3.E-03	4.E-04	1.E+02	6.E-05
Intersect spacer upper	8.E-02	2.E-03	8.E-04	1.E+02	1.E-04
Intersect Top	9.E-03	2.E-03	7.E-03	1.E+03	1.E-03
inlet_pipe	2.E-02	9.E-04	2.E-03	2.E+02	3.E-04
inlet_pipe2	1.E-03	6.E-05	4.E-04	2.E+01	7.E-05
Average	**3E-02**	**1E-03**	**5E-03**	**7E+02**	**8E-04**

Table 2 Estimation of turbulent length-scales in the inertial and energy containing subrange

Given the two parameters, ε and υ, respectively the turbulent kinetic energy dissipation rate and the kinematic viscosity of the lead, there are (to within multiplicative constant) unique length, velocity and time scales that can be formed, and these are the Kolmogorov scales:

$$\eta \equiv \left(\frac{\upsilon^3}{\varepsilon}\right)^{\frac{1}{4}} \tag{2}$$

$$u_\eta \equiv (\upsilon\varepsilon)^{1/4} \tag{3}$$

$$\tau_\eta \equiv \left(\frac{\upsilon}{\varepsilon}\right)^{1/2} \tag{4}$$

Fuid volume	Volume Average of Turbulent Dissipation Rate ε [m²/s³]	Volume Average of Turbulent Kinetic Energy k [m²/s²]	Kolmogorov Scales		
			lenght η $(\nu^3/\varepsilon)^{1/4}$ [m]	velocity u_η $(\nu\varepsilon)^{1/4}$ [m/s]	time τ_η $(\nu/\varepsilon)^{1/2}$ [s]
bottom_vol	3.E-04	7.E-05	8.E-05	6.E+00	3.E-02
Esa+cyl_layer	1.E-01	3.E-03	2.E-05	3.E+01	1.E-03
Esa_channel	1.E-01	1.E-03	2.E-05	3.E+01	1.E-03
Fluid slice 2 middle low	1.E-01	3.E-03	2.E-05	3.E+01	1.E-03
Fluid slice 3 middle central	6.E-02	1.E-03	2.E-05	2.E+01	2.E-03
Fluid slice 4 middle up	6.E-02	1.E-03	2.E-05	2.E+01	2.E-03
fluid_slice_1_new	8.E-02	1.E-03	2.E-05	2.E+01	2.E-03
Intersect spacer lower	4.E-01	3.E-03	1.E-05	4.E+01	7.E-04
Intersect spacer upper	8.E-02	2.E-03	2.E-05	2.E+01	2.E-03
Intersect Top	9.E-03	2.E-03	3.E-05	1.E+01	5.E-03
inlet_pipe	2.E-02	9.E-04	3.E-05	2.E+01	4.E-03
inlet_pipe2	1.E-03	6.E-05	5.E-05	9.E+00	1.E-02
Average	**3E-02**	**1E-03**	**2E-05**	**2E+01**	**3E-03**

Table 3 Estimation of Kolmogorov length scales

The base size of the mesh implemented by STARCCM+ mesher is equal to 1 mm. This is confirmed by the simplest method proposed in literature for the estimation of the resolved eddy length scales, which is based on the mesh size. This method proposes the calculation of the average volume of the fluid volume that composes the fluid domain and then estimates the length scales by

$$\ell_{mesh} = \sqrt[3]{V} \tag{5}$$

confirming that the base size already introduced was the average length scale resolved by the LES model based on the implemented mesh.

Another important parameter to assess the quality of the calculations is related to the characteristic wavenumber, generally defined as

$$k_\ell = \frac{2\pi}{\ell} \tag{6}$$

Finally, another important parameter, that qualifies the time discretization in terms of good or poor accuracy and causing the divergence of the calculus if their value exceed the unity, rigorously spoken, is the Courant number (Courant-Friedrichs-Lewy conditions, CFL) defined as, in the n-dimensional case,

$$CFL\ conditions: \sum_1^n \frac{u_i\,\Delta t}{\Delta x_i} < 1 \tag{7}$$

Where u_i is the component of velocity in the i-direction, Δx_i is the space in the i-directions (CFD-spoken, the length of the fluid volume side in the i-direction) and Δt is the time integration step. These conditions cause a severe limitations for the time-step choice: however, most of the CFD codes, with the implicit time discretization, tolerate value of CFL < 10-20. In this case, with the time step imposed equal to 3E-04 s, a very good respect of the CFL conditions has been reached, as shown in Table 4.

range	#cells	%
0 < CFL < 1	1.51E+06	96.91
1 < CFL <5	4.80E+04	3.08
CFL > 5	1.55E+02	0.01
TOT	1557276	100.00

Table 4 CFL conditions volume report with time step size equal to 3E-04 s

In Table 5 are reported the comparisons among the calculated length, time and wavenumber scales with eq. (1) – (6) and the value obtained with the computational grid performed and the imposed time step size. The Large Eddy Turn-Over Time, that is referred at the largest eddy in the flow (that account the most of the transport of momentum and energy), can be simply estimated by

$$LETOT = \frac{\ell_0}{u_{mean}} \tag{8}$$

where ℓ_0 is the integral length scale and u_{mean} the mean velocity of the flow. Assuming this mean velocity equal to that in mixing region, we have LETOT ~ 1E-02 s, then the simulation time performed (20 s) is enough (~ 1000 LETOT).

Scale	*ℓ [m]*	*τ[s]*	*kc [1/s]*
Energy containing range	5E-003	4E-002	1E+003
Inertial sub-range	8E-004	1E-002	8E+003
Kolmogorov	2E-005	3E-003	3E+005
LES-14Mnodes	1E-003	3E-004	6E+003

Table 5 Turbulent length scales theoretical and CFD grid-based comparison

The calculated average length scales in the whole domain are:

- Δx^+(spanwise)~40 ($30<\Delta x^+<65$);
- y^+(near wall)~1;
- Δz^+(streamwise)~120 ($80<\Delta z^+<220$);

It's possible to note that:

- the time step selected is satisfactory;
- the length is not totally in the inertial subrange, but is acceptable.

LES calculations require a lot of computational resources, both in terms of RAM and processor availability.
The first is almost controlled by the mesh size: in this case, with about 32 Gb of memory are required.

From the point of view of the processor availability, the influencial parameter is the calculation time: serial processor with this size of mesh and time step of order 1E-04 s would require several months, or even a few years, for reaching the required convergence.
In this case, a parallel 400-way MPI run was performed, with a calculation time (to simulate 20 s of transient, i.e about 66500 time steps) approximately of a month.
In Table 6 are reported the numerical setting for LES turbulence models calculation. The BCs are the same of the URANS case.

Turbulence model	Large Eddy Simulation
Subgrid treatment	WALE
Wall treatment approach	Two layer All y+
Time discretization	Implict 2nd order
Convection discretization	2nd order
	Segregated Flow
Solutions Methods	Segregated Fluid Temperature
	Segregated Solid energy

Table 6 Numerical schemes for LES calculation

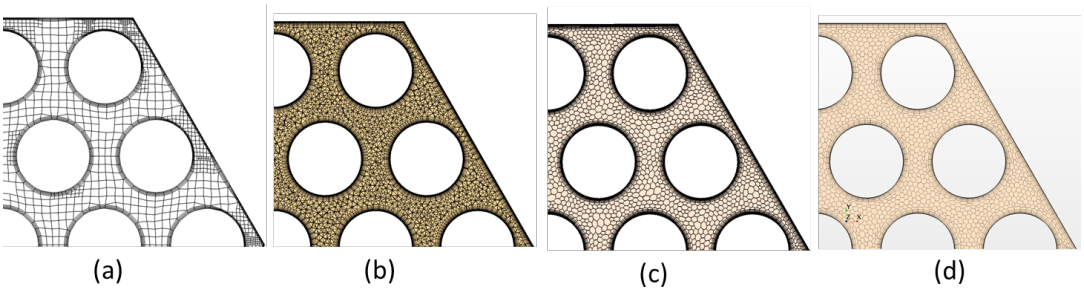

Figure 5 Sketches of the mesh developed: Polimi (a) , ENEA (b) , NRG (c) , Unige/CRS4 (d)

3.3Comparison set-up

Due to the engineering purpose of this study, only pragmatic probes and variable trends are compared. Four comparisons are distinguished:

1. Velocity components (v_x , v_y, v_z) and temperature on two lines in the centre of different subchannels (see Figure 6-left-): one over the blockage (B2) and one over an unblocked one (E2).
2. Temperature on two axial lines on different pin surfaces (indicated by orange rhombuses in Figure 6-left-): one on a pin affected by the blockage (pin 5), one on an undisturbed pin (pin 2).
3. Temperature on three axial lines located into the mixing region (Figure 6-right-): one on the z axis (pipe center line, yellow cross), one over the blockage (red cross), one over an undisturbed sector (non-blocked, green cross).
4. Temperature on three radial lines (bisector line of sectors B and E -wall to wall line-) located into the mixing region at different axial location: at the beginning of the mixing region (0.95 m), at its middle height (1.1 m), at the outlet section of the model.

Figure 6 Sketch of the BFPS test section (edge blockage is performed on sector B) with monitored subchannels (in red) and pins (in orange) on the left. Sketch of the axial lines in the mixing region (on the right); grid holes (unblocked) are also reported in black to illustrate the blockage location.

4. RESULTS: COMPARISON OF DIFFERENT APPROACHES

Looking for a blank reference comparison (without blockage effects) between the different simulations, subchannel E2 (central subchannel, far from the blockage) was selected. Velocity components and temperature are extrapolated at the centre of the sub-channel, results from the different simulations are shown in Figure 7. The axial trend of the temperature shows the same slope for all the simulations. Overall, the computed temperature is within 5 °C for all CFD approaches. In the same figure, the axial profiles of the secondary velocity components along the x (b) and y (c) axes are shown, the different simulations predict the same length of disturbance behind the grid and at least the same axial distance of the velocity minimum (except for URANS-Unige/CRS4- results of velocity y) while their absolute values are really scattered and can double from a simulation to the other. The length of disturbance highlighted by the codes shows that also a free sub-channel far from a blockage, as E2, is affected by its interference. The axial velocity component (velocity z) shows the same features, all the RANS and URANS simulations overestimate the velocity trend into the disturbance length compared to the preliminary LES results, in particular the URANS-Unige/CRS4 simulation overestimates it showing a "step behaviour" in the first 0.1 m and a wavelike behaviour in the rest while all the other simulations show an asymptotic trend to an average sub-channel velocity (0.56 m/s), slightly under-estimated by ENEA/Unipi and NRG (0.54 m/s) compared to the preliminary LES results. That "step-behaviour" is also observed by Polimi.

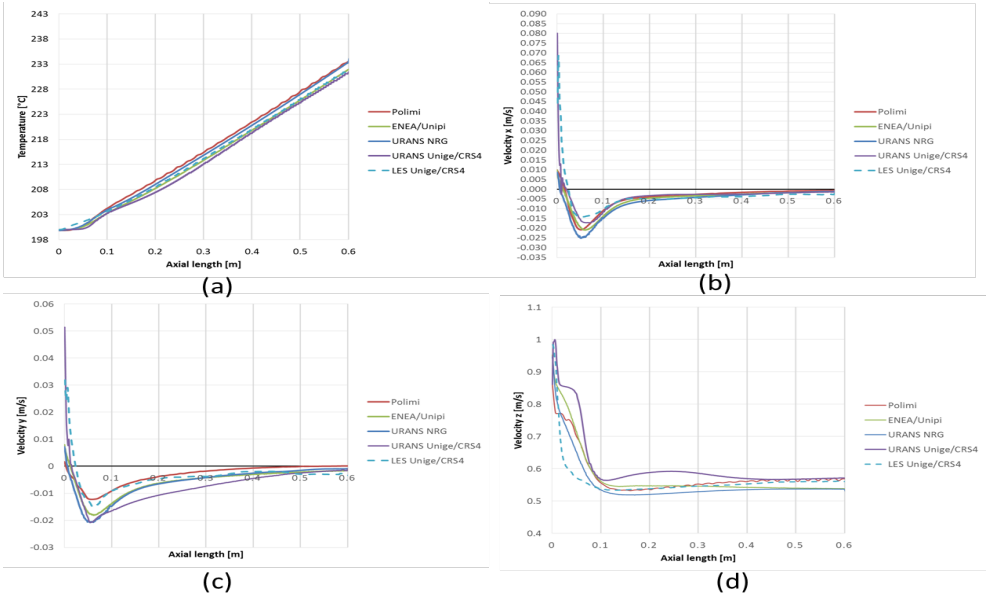

Figure 7 Comparison of temperature (a) and velocity components: velocity x (b) , velocity y (c) and main velocity z (d), predicted by different codes in subchannel E2.

The comparison of the velocity components and temperature in the blocked sub-channel B2 is provided in Figure 8. With reference to the axial temperature trend (a), the peak temperature immediately behind the blockage shows at least the same axial distance for all the simulations while its value is considerably different for each simulation with RANS and URANS simulations that overestimate it compared to the preliminary LES results and ranging from Polimi (263°C) to ENEA/Unipi (245°C), URANS-Unige/CRS4- (240°C), URANS NRG (234 °C), and LES value (224 °C). The axial temperature trend behind the disturbance length shows two different trends with the same slope: a lower trend (for URANS and RANS simulations) and LES higher trend. Looking at the secondary velocity components (b) and (c) in Figure 8, while their general slope is fully captured by all the simulations, their maxima and minima

are considerably scattered, in particular for velocity y (c) the ENEA/Unipi slope predicts a lower cross-flow compared to the others while the two URANS predict the same minimum value. Finally, the axial slope of the main-stream velocity z is plotted in Figure 8(d) where the same three trends of the temperature slope can be recognized : the higher one (Polimi), the average one (ENEA/Unipi and URANSs) and the lower one (LES). In the same graph, ENEA/Unipi minimum velocity in the disturbance length matches LES results and the two URANS simulations show the same trend and values.

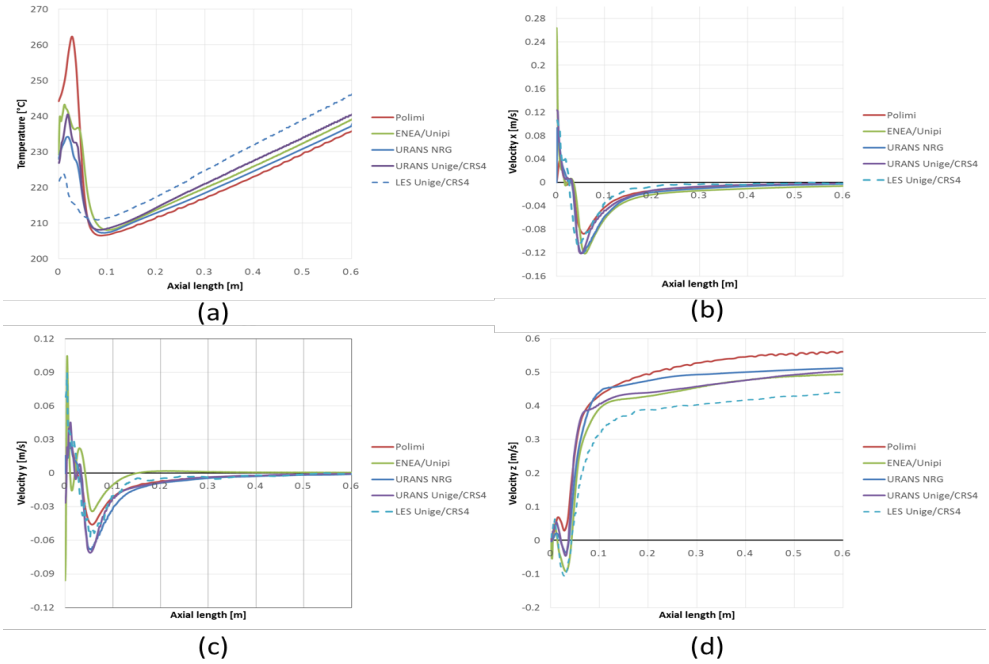

Figure 8 Comparison of temperature (a) and velocity components: secondary velocity x (b) , secondary velocity y (c) and main velocity z (d), predicted by different codes in subchannel B2

Axial temperature trends on pin2 (unblocked) and pin5 (blocked) are shown in Figure 9. The axial temperature trends on pin2 are in good agreement even if RANS and URANS results underestimate the temperature values compared to the preliminary LES (URANS by NRG is the most similar to it). Looking at the axial temperature trend on pin 5 (located over the blockage), RANS and URANS simulations over-estimate the peak temperature if compared to the preliminary LES results; in particular we can find the same trend of sub-channel B2 axial temperature (Figure 8 -a-).

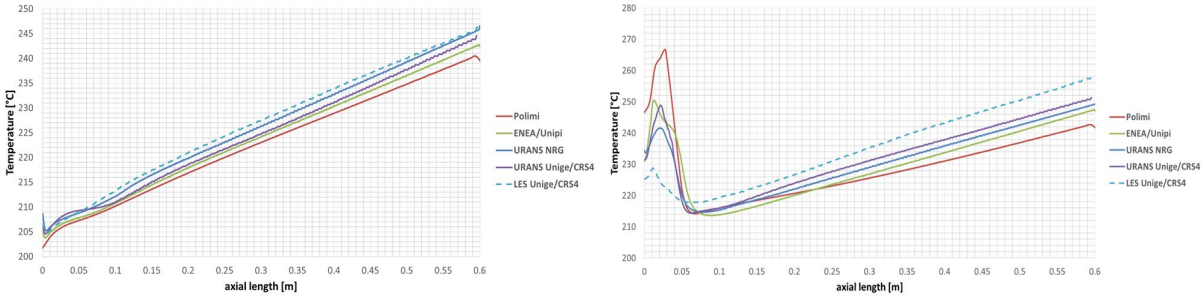

Figure 9 Comparison of axial temperature trend on pin 2 (left - undisturbed subchannel) and pin 2 (right - over the blockage).

Finally, comparing temperature trends on axial and radial lines into the mixing region (Figure 10), the axial trends on the central line (top center figure) show similar trends for RANS and URANS simulations

(ENEA/Unipi and NRG URANS are almost similar) and a completely different trend for the preliminary LES. The axial trends over the free subchannels (top left of Figure 10) show a similar slope (ΔT) for RANS and URANS simulations while the temperature ranges are completely different. The axial trends over the blockage (top right of Figure 10) show the same slope for all RANS and URANS simulations but none is in accordance to the preliminary LES results This implies that the mixing modeling of the different codes is similar and leads to similar trends, though the absolute values are different.
Regarding the temperature trends on the three radial lines located at different heights (bottom of Figure 10), both RANS and URANS simulations show the same trends with a remarkable temperature difference (about 9 °C) between the area over the blockage (positive value of radial length) and the one over the free subchannels (negative values of radial length) confirming the feasibility of a temperature monitoring system for flow blockage detection. Otherwise, the preliminary LES results show the same temperature difference in radial direction but predict a completely different slope.

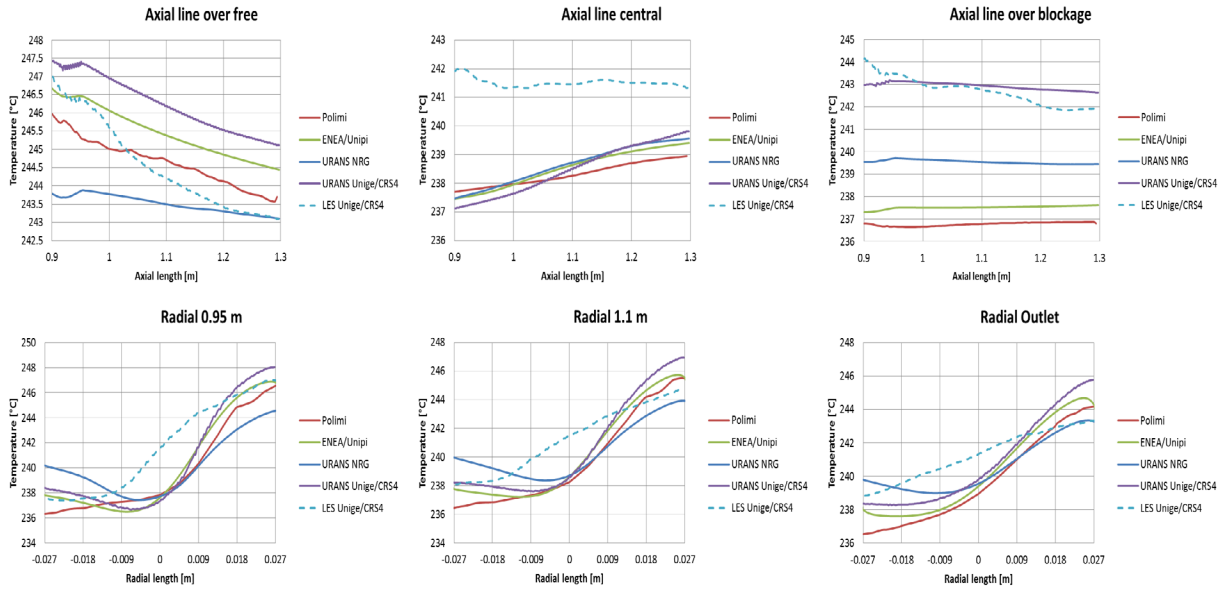

Figure 10 Comparison of temperature trends in the mixing region. Axial lines on the top, radial streamlines at the bottom (positive values of radial length indicates the zone over the blocked sub-channels).

5. CONCLUSIONS

The present paper is focused on the CFD modelling and preliminary computational analysis of the new experimental facility 'Blocked' Fuel Pin bundle Simulator (BFPS) that will be inserted in the heavy liquid metal NACIE-UP (NAtural CIrculation Experiment-UPgrade) facility located at the ENEA Brasimone Research Center (Italy). The BFPS test section aims to carry out suitable experiments to fully investigate different flow blockage regimes in a 19-pin fuel bundle providing experimental data in support of the development of the ALFRED (Advanced Lead-cooled Fast Reactor European Demonstrator) LFR DEMO.
The thermal-hydraulics of the new BFPS test section is analysed for one relevant blockage with different CFD codes and different approaches. All general trends are well captured by RANS and URANS simulations even if there is a remarkable difference between the exact values of these trends (in particular their maxima and minima).
It is relevant that results show a good agreement among the different codes/approaches on the extension of the recirculation region behind the blockage, the position of the local maxima/minima and the mixing downstream the bundle. However, care should be taken with drawing conclusions, since the provided LES results are preliminary.

A more detailed comparison with an improved LES computation is foreseen. Besides, experimental data of the temperature will be produced in the NACIE-UP facility at ENEA, so a second thermal verification can be envisaged.

ACKNOLEDGEMENT

This work was performed in the framework of the H2020 SESAME project. This project has received funding from the Euratom research and training programme 2014-2018 under grant agreement No 654935.

REFERENCES

1. G.F. Schultheiss, “On local blockage formation in sodium cooled reactors”. *Nuclear Engineering and. Design*, **100**, pp. 427-433 (1987).
2. Seung-Hwan Seong, “Establishment of the design requirements for a flow blockage detection system through a LES analysis of the temperature fluctuation in the upper plenum”, *Annals of Nuclear Energy* , **33**, pp. 62-70, (2006).
3. R.K. Maity, K. Velusamy, P. Selvaraj, P. Chellapandi, “Computational fluid dynamic investigations of partial blockage detection by core-temperature monitoring system of a sodium cooled fast reactor”, *Nuclear Engineering and. Design,* **241**, pp. 4994-5008 (2011).
4. I. Di Piazza, F. Magugliani, M. Tarantino, A. Alemberti, “A CFD analysis of flow blockage phenomena in ALFRED LFR demo fuel assembly”, *Nuclear Engineering and. Design,* **276**, pp. 202–215 (2014).
5. I. Di Piazza, M. Angelucci, R. Marinari, M. Tarantino, N. Forgione, “Heat transfer on HLM cooled wire-spaced fuel pin bundle simulator in the NACIE-UP facility”, *Nuclear Engineering and. Design,* **300**, pp. 256-267 (2016).
6. G. Grasso,C. Petrovich,D. Mattioli,C. Artioli,P. Sciora,D. Gugiu G. Bandini,E. Bubelis,K. Mikityuk,"The core design of ALFRED, a demonstrator for the European lead-cooled reactors", *Nuclear Engineering and Design*, **278**, pp. 287-301 (2014).
7. I. Di Piazza, R. Marinari, “CFD PRE-TEST ANALYSIS OF THE FUEL PIN BUNDLE SIMULATOR EXPERIMENT IN THE NACIE-UP HLM FACILITY”, 16th International Topical Meeting on Nuclear Reactor Thermal - Hydraulics, NURETH-16, August 30-September 4, Hyatt Regency Chicago (2015).
8. H.J. Doolaard, A. Shams, F. Roelofs, K. Van Tichelen, S. Keijers, J. De Ridder, J. Degroote, J. Vierendeels, I. Di Piazza, R. Marinari, E. Merzari, A. Obabko, P. Fischer, “CFD BENCHMARK FOR A HEAVY LIQUID METAL FUEL ASSEMBLY” 16th International Topical Meeting on Nuclear Reactor Thermal - Hydraulics, NURETH-16, August 30-September 4, Hyatt Regency Chicago (2015).
9. OECD/NEA, “Handbook on Lead-bismuth Eutectic Alloy and Lead Properties, Materials Compatibility, Thermal-hydraulics and Technologies” (2007)
10. D. Martelli, R. Marinari, G. Barone, I. Di Piazza, M. Tarantino, “CFD thermo-hydraulic analysis of the CIRCE fuel bundle”, *Annals of nuclear energy,* **103**, pp. 294-305 (2017).